



One Ring to Rule Them All: An Open Source Smartring Platform for Finger Motion Analytics and Healthcare Applications

Hao Zhou*

hfz5190@psu.edu

The Pennsylvania State University
USA

Taiting Lu*

txl5518@psu.edu

The Pennsylvania State University
USA

Yilin Liu

yzl470@psu.edu

The Pennsylvania State University
USA

Shijia Zhang

scarlettzhang27@psu.edu

The Pennsylvania State University
USA

Runze Liu

rml6043@psu.edu

The Pennsylvania State University
USA

Mahanth Gowda

mahanth.gowda@psu.edu

The Pennsylvania State University
USA

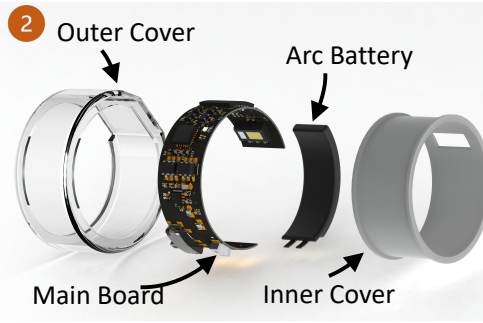


Figure 1: *OmniRing* is designed by integrating low-cost off-the-shelf electronic components based on SoC architecture into a flexible PCB that can bend in the form factor of a ring. IMU and PPG sensors are embedded for enabling motion analytics and healthcare applications. The hardware is enclosed in a 3D-printed waterproof case that allows smooth contact with the skin. Overall form factor weighs about 2.5 g with a week of battery life for comfortable and long-term wearing including while sleeping and swimming.

ABSTRACT

This paper presents *OmniRing*, an open-source smartring platform with IMU and PPG sensors for activity tracking and health analytics applications. Smartring platforms are on the rise because of comfortable wearing, with the market size expected to reach \$92 million soon. Nevertheless, most existing platforms are either commercial and proprietary without details of software/hardware or use suboptimal PCB design resulting in bulky form factors, inconvenient for wearing in daily life. Towards bridging the gap, *OmniRing* presents an extensible design of a smartring with a miniature form factor, longer battery life, wireless communication, and water resistance so that

users can wear it all the time. Towards this end, *OmniRing* exploits opportunities in SoC, and carefully integrates the sensing units with a microcontroller and BLE modules. The electronic components are integrated on both sides of a flexible PCB that is bent in the shape of a ring and enclosed in a flexible and waterproof case for smooth skin contact. The overall cost is under \$25, with weight of 2.5g, and up to a week of battery life. Extensive usability surveys validate the comfort levels. To validate the sensing capabilities, we enable an application in 3D finger motion tracking. By extracting synthetic training data from public videos coupled with data augmentation to minimize the overhead of training data generation for a new platform, *OmniRing* designs a transformer-based model that exploits correlations across fingers and time to track 3D finger motion with an accuracy of 6.57mm. We also validate the use of PPG data from *OmniRing* for heart rate monitoring. We believe the platform can enable exciting applications in fitness tracking, metaverse, sports, and healthcare.

*Co-primary authors

Project page: <https://www.cse.psu.edu/~mkg31/projects/omniring/>

Permission to make digital or hard copies of all or part of this work for personal or classroom use is granted without fee provided that copies are not made or distributed for profit or commercial advantage and that copies bear this notice and the full citation on the first page. Copyrights for components of this work owned by others than the author(s) must be honored. Abstracting with credit is permitted. To copy otherwise, or republish, to post on servers or to redistribute to lists, requires prior specific permission and/or a fee. Request permissions from permissions@acm.org.

IoTDI '23, May 9–12, 2023, San Antonio, TX, USA

© 2023 Copyright held by the owner/author(s). Publication rights licensed to ACM.

ACM ISBN 979-8-4007-0037-8/23/05...\$15.00
<https://doi.org/10.1145/3576842.3582382>

ACM Reference Format:

Hao Zhou, Taiting Lu, Yilin Liu, Shijia Zhang, Runze Liu, and Mahanth Gowda. 2023. One Ring to Rule Them All: An Open Source Smartring Platform for Finger Motion Analytics and Healthcare Applications. In *International Conference on Internet-of-Things Design and Implementation (IoTDI '23)*, May 9–12, 2023, San Antonio, TX, USA. ACM, New York, NY, USA, 12 pages. <https://doi.org/10.1145/3576842.3582382>

1 INTRODUCTION

Sensor-embedded smartwatches are being envisioned for many applications in the areas of fitness tracking, gesture analytics, and healthcare [35, 36]. Consequently, the market size is booming and is expected to reach \$92 million in the next few years [3]. Multiple popular commercial products are available on the market [64] such as OuraRing [57] which tracks sleep, stress, activity levels, etc. In contrast to sensor embedded gloves [2] or strap [9] based platforms that are known to cause discomfort and preclude precise finger motion [62], rings can be designed in aesthetic and ergonomic form factors, that are comfortable to wear and allow natural finger motion, as validated by a recent user experience study [20]. Moreover, since there is no display like smartwatches and the advent of low power microcontrollers, a longer battery life can be supported, thus making it possible to wear them all the time including sleeping and swimming. This offers a platform with deeper and more intimate levels of sensing information.

Towards this end, this paper designs a smartring platform called *OmniRing* with embedded sensors with the following requirements: (i) Aesthetically pleasing appearance and form factor with small weight and size. (ii) Longer battery life (iii) Wireless communication with a smartphone app for streaming raw sensor data for analytics (iv) Ability to cover a wide array of sensing applications. (v) Water resistance (vi) Extensibility to add additional sensors (vii) Low cost.

Prior works in the academic community [9, 43, 48] do not satisfy all of the above requirements either due to suboptimal PCB designs resulting in bulky form factors or due to lack of wireless communication resulting in wired prototypes making it hard to wear in daily life. On the other hand, commercial products available on the market satisfy most of the above requirements. However, their platform is closed without any details about the software or hardware. For example, none of the internal details of the hardware and electronics of OuraRing platform is publicly available, and there are no APIs that allow the developers to access the raw sensor data. In contrast to such works, we design our platform to satisfy all of the requirements above while sharing full details of hardware, software, and firmware. We will open-source our platform with this paper for the community to develop interesting use cases.

Towards satisfying the above requirements, Fig. 1 depicts *OmniRing* design. We leverage innovations in system-on-chip (SoC) architecture to integrate computing and wireless communication into a small chip and also exploit advances in printed circuit board (PCB) design by printing the circuit on both sides of a flexible printed circuit board (FPCB) that is bent in the shape of a ring. We incorporate inertial measurement unit (IMU) and photoplethysmography (PPG) sensors that can enable a wide range of applications in motion analytics (IMU) and healthcare (PPG + IMU). The entire electronics is embedded in a 3D-printed waterproof case designed using a combination of Resin and Thermoplastic Polyurethane (TPU) materials that provide smooth contact with the skin surface, thus allowing long-term and comfortable wearing. The PCB

was assembled using commercial-off-the-shelf (COTS) electronic components and printed using a self-assembly PCB manufacturer, thus keeping the overall manufacturing cost under \$25 with an overall weight $\approx 2.5\text{g}$ which is even lighter than the commercial OuraRing [57]. With the use of the COTS components and low-cost manufacturing techniques, we believe this allows new designers and developers to extend *OmniRing* to incorporate additional capabilities.

To validate *OmniRing* in the context of a real-world use-case, we develop a concrete application of 3D finger motion tracking, which can enable exciting applications in the areas of augmented and virtual reality (AR and VR) [53, 56], sports analytics [32], sign languages [74], smart healthcare, etc [37, 38]. In contrast to camera-based approaches [1, 6] that can be privacy sensitive and need good lighting and resolution, wearable sensors like *OmniRing* can offer solutions that are privacy-agnostic and work anywhere including heavy occlusions or outdoors where the user is constantly moving.

Such 3D tracking is challenging for many reasons: (i) Search space for 3D finger pose is large (*24 degrees of freedom, DoF*) and tracking them without sensors on all fingers is an underconstrained problem without closed-form equations. To address this, *OmniRing* takes a learning based approach that exploits the inter-finger correlations to fill the gaps in sensing and automatically learns the mapping between sparse sensor data and 3D finger motion. (ii) To train the above ML models, there are no large-scale high-quality training datasets because creating such datasets is expensive and time-consuming [41, 46]. This is particularly true for newly developed wearable platforms like *OmniRing*. Motivated by recent success in harvesting synthetic training data from videos [46, 51], we adopt a similar approach. However, in contrast to prior works (i.e., IMUTube [46], ZeroNet [51]) that classify 10-50 predefined gestures, *OmniRing* tracks continuous 24 DoF finger motion. Furthermore, data augmentation techniques are designed to handle the domain difference between real and synthetic data and develop robustness to diversity across users and variation in sensor position, orientation, etc. To the best of our knowledge, *OmniRing* is the first work to harvest synthetic training data from videos for solving a problem where the search space is continuous finger motion. We believe this will bootstrap many applications in sign language recognition, smart healthcare, etc, where collecting training data is challenging.

A user experience study is conducted, in which *OmniRing* satisfies the users with high ratings across multiple dimensions such as comfort, appearance, and weight, suggesting the increasing acceptability of such ring-based form factors in daily life. For validating finger motion performance, a systematic study with diverse users achieves a joint position accuracy of 6.57mm and the joint angle accuracy of 8.68° . The accuracy is consistent over finger joints, various users, and longer durations of free-living experiments. Examples of qualitative reconstruction results are shown in Fig. 13.

We enumerate our contributions below: ■ Design of a sensor-embedded smartring by exploiting innovations in flexible PCB, 3D printing, and low-cost manufacturing to enable continuous sensing with long battery life and small form factor for diverse

applications in motion analytics and healthcare. ■ Demonstrated the feasibility of extracting training data from public videos for 3D finger motion tracking with *OmniRing*, and development of a *transformer*-based architecture that identifies opportunities in inter-finger correlations for tracking all fingers without the need to place sensor rings on all fingers. ■ Conducted a systematic user study to validate the comfort levels and acceptance of *OmniRing* in daily life as well as validating the performance of 3D finger motion tracking with robustness to user diversity, changes in sensor position, and ability to perform under free living conditions. ■ We will open-source *OmniRing* for the community to extend it with novel capabilities in hardware and applications.

2 RELATED WORK

Wearable Sensing Platforms: While sensor-embedded gloves are popular for gesture recognition with IMU, flex, and capacitive sensors [16], prior studies note that wearing gloves precludes the user from performing activities requiring fine precision because they can hinder natural dexterous hand motion [62]. Strap-based sensors [9, 84] might be another alternative. However, they limit the mobility of the hand because different fingers are bound by straps. In contrast, *OmniRing* uses sensor-embedded rings that allow natural finger motion activities and are comfortable for wear during activities including sleeping and swimming. EMG sensors are used for finger tracking [50, 52], but they need calibration and warming of the skin to be in proper contact with the electrodes which takes up to 5 minutes during each instance of wearing, leading to usability issues. Wrist-based sensing including capacitive [71], inertial, and acoustic sensors [18] is popular for hand motion recognition. However the recognition is limited to discrete gestures, thus limited in capturing 3D finger motion.

Smartring Platforms: DualRing uses IMU sensors on the fingers to classify nine discrete gestures [48]. However, the sensors are connected by a wire for data collection which can limit comfortable usage for a long time. TypingRing [55] detects typing activities based on IMU sensors placed on the finger. However, the sensor is bulky in size because the development boards are directly connected to each other without carefully compressing them into a PCB. AuraRing [58] uses a magnetic ring for tracking finger motion by sensing the magnetic field changes at the wrist. In contrast, *OmniRing* implements the entire sensing and SoC logic on the ring as opposed to sensing magnetic field at the wristwatch thus allowing extensibility to incorporate additional sensors like PPG by offering a fully self-contained smartring platform. Similarly, several ring-based platforms that include various modes of sensing such as IMU, temperature, pressure, and ECG have been designed as outlined in a recent survey paper [73]. However, most of these platforms are either bulky due to suboptimal PCB design, not easily wearable for a long time due to choice of material and lack of water resistance, or need to be connected via a wire for data access, and so on. The commercially available OuraRing [57] is perhaps the closest to our platform. However, the technical details are closed due to the proprietary nature of

the hardware and there is no access to the raw sensor data for developers. To the best of our knowledge, *OmniRing* is the first opensource platform that satisfies all of the requirements outlined in the second paragraph of Sec. 1.

Cameras: Related to 3D finger tracking in *OmniRing*, depth cameras like Kinect [6] and Leap [1] can also track 3D finger motion. Even monocular RGB cameras can capture the 3D finger motion [23, 26, 53]. While such works are transformative, cameras are known to be privacy-invasive, they require the user to be in view of the camera, and they need good lighting and resolution. This might be impractical in settings with heavy occlusions or outdoors where the user is continuously moving. Digits [44] and DorsalNet [80] use wrist-mounted visual and infrared cameras for 3D finger pose tracking. However, the camera needs to sit high enough on the wrist or even reach the palm to capture the full range of finger motion. FingerTrak [40] uses wearable thermal cameras to track finger motion, but the system is not robust to background temperatures (sun, heater, etc) and changes in sensor position due to wrist motion. In contrast, *OmniRing*'s solution is ubiquitous while being robust to ambient conditions (occlusions, lighting) and natural variation in sensor positions and wrist motions.

Harvesting Training Data from Videos: Synthetic data from motion capture videos (like ViCON [75]) is used for training body pose tracking algorithms with 6 IMUs [41]. In contrast to high-fidelity ViCON cameras and body motion tracking, *OmniRing* uses low-fidelity videos and performs finger motion tracking. *OmniRing* is inspired by recent works like IMUTube [46] which extracts training data from YouTube videos for activity classification (walking, running, sitting, etc). In contrast to full-body activity classification, *OmniRing* solves a different problem of 3D finger motion tracking. Other innovative works [47, 68, 70, 83] have also explored the use of videos for training human activity recognition and gesture classification. Work in [61] extracts 2D pose from videos for classifying 10 exercises. Similarly, the work [51] classifies 50 sign language gestures. In contrast to such works that classify predefined gestures of motion activities (running, sitting, eating, waving, etc.), *OmniRing* performs 3D tracking of completely arbitrary finger motion which could be used in any applications like AR/VR, sign language recognition, etc.

3 THE OMNIRING PLATFORM

In this section, we describe the platform design of *OmniRing* with embedded IMU and PPG sensors and BLE communication for motion analytics and healthcare applications. First, we elaborate on the design principles of *OmniRing*. Later, we describe the design of the form factor, hardware, and software.

3.1 Design Principles

Our main objective when developing the *OmniRing* platform was to provide a general-purpose hardware sensing platform for the wearable research community that allows for the exploration of state-of-the-art sensing capabilities on ring form factor devices. We were guided by the following principles throughout the design and development process.

Aesthetics and Social Acceptance: *OmniRing* must be lightweight and have a good appearance to receive better social acceptance. Commercial platforms like OuraRing [57] and FinchRing [33] have gained favorable reviews online [4], an extensive in-situ usability study conducted recently using a mock ring [20] has validated the acceptance by users for continuously wearing rings for applications in activity monitoring, user interfaces, mobile payments, and healthcare. These studies indicate that ring-based form factors have attracted a lot of attention recently because users are comfortable wearing them all the time. Therefore, *OmniRing* is designed in the form factor of a lightweight ring.

Longer Battery Lifetime and Easy Recharging: Long battery life enables continuous monitoring of users' activity and health metrics including sleep monitoring. *OmniRing* should be easy and convenient to be recharged periodically. *OmniRing* is designed using a low-power microcontroller that can monitor the sensors with up to a week of battery life before recharging.

Wireless Communication: The *OmniRing* platform should be portable and wireless to transmit data to a smartphone, so that users can access data anywhere and anytime. Furthermore, the data can be processed with powerful AI algorithms on edge devices for analytics. *OmniRing* is designed with a SoC with integrated BLE with low-power requirements and a small size.

Coverage of a Wide Range of Applications: The small form factor of a ring does not allow embedding many sensors. Thus, we only embed IMU and PPG sensors with complementary sensing abilities. While IMU provides motion analytics applications like activity detection, augmented reality, and sports analytics, the PPG sensor enables healthcare applications like heart rate and blood pressure monitoring [15], emotion and sleep sensing [42]. Thus, we believe the choice of sensors supports diverse applications in motion analytics and healthcare.

Water Resistance: The platform should be waterproof to protect against adverse environmental conditions like rain and snow and allow analytics during water sports and swimming. Furthermore, the material that interfaces with the skin surface must be comfortable for long-term wearing. The materials for enclosing the electronics are carefully chosen and 3D-printed with appropriate shape to satisfy this requirement.

Openness and Extensibility: *OmniRing*'s hardware and software platform should be easily extensible by the research community. Because of the requirements of a small form factor, the current version of *OmniRing* only integrates IMU and PPG sensors which can still cover a diverse range of motion analytics and healthcare applications. However, other sensors such as temperature, ECG, and ultrasonic sensors can be included depending on the requirements of an application. We believe open sourcing *OmniRing* will promote extensibility.

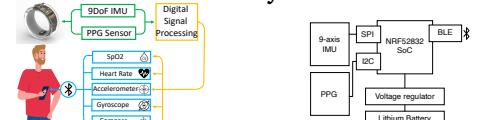
Manufacturability and Cost-Effectiveness: In order for the community to leverage the *OmniRing* platform for research, they must be able to easily manufacture the device at an affordable cost. To achieve this, we focused on low-cost commercial off-the-shelf (COTS) electronic components. These components would be integrated into a custom PCB, specifically designed to be manufactured, and components assembled, by a self-service PCB assembly manufacturer at a nominal cost.

3.2 Platform Design

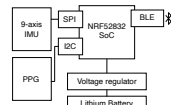
Form Factor Design: Our goal is to design a lightweight, waterproof and comfortable ring that can be worn throughout the day and night while being embedded with electronics and sensors that can sense the user activity, heart rate, etc., and stream the data wirelessly for analytics, as depicted in Fig. 3a. While prior works adopt certain

electronic components [43, 48] that can provide rapid prototyping, this results in a bulky form factor because such components when combined together can be suboptimal for the overall device size. Therefore, we exploit the following opportunities to decrease the form factor size while satisfying the requirements of embedded sensing and electronics. (i) We design the electronics using a FPCB that we bend in the shape of a ring. We assemble a custom microcontroller and sensing hardware into the FPCB, the details will be elaborated shortly. We also integrate a battery in the shape of an arc into the ring (Fig. 1) to power the hardware. (ii) We enclose the hardware inside a waterproof case, the material of which is comfortable for skin contact and long-term wearing. We selected clear resin material using Stereolithography (SLA) 3D printing technology for an optically clear, stable, and aesthetically pleasing appearance. The inner ring is designed to fit a particular user's finger size and developed using fused deposition modeling (FDM) technology with TPU materials for flexibility and comfortable skin contact. The overall form factor is depicted in Fig. 1, it weighs between 2.5-2.8g depending on finger sizes and is comparable to the commercially available OuraRing which weighs 4-6g [57].

Hardware and Power Circuitry: Given the small size of the



(a) Overview of *OmniRing*



(b) Hardware Architecture

Figure 3: Usage and Hardware Architecture Design of *OmniRing*
 Figure 3 illustrates the usage and hardware architecture of *OmniRing*. The usage diagram (a) shows a person wearing the ring, which contains a 9Dof IMU, a PPG Sensor, and a Digital Signal Processing unit. The ring also includes sensors for SpO2, Heart Rate, Accelerometer, Gyroscope, and Compass. The hardware architecture (b) shows the internal components: a 9-axis IMU, a PPG sensor, a digital signal processing unit, an NRF52832 SoC, a BLE module, an I2C interface, a voltage regulator, and a lithium battery. The IMU and PPG are connected to the digital signal processing unit, which then connects to the NRF52832 SoC. The SoC is connected to the BLE module, I2C, and voltage regulator. The voltage regulator powers the SoC and the lithium battery. The form factor as discussed above, the main challenge would be to embed the following hardware components within the limited space. (i) Sensing hardware which includes IMU and PPG sensors in the current edition of *OmniRing* (ii) A microcontroller (MCU) to assemble the data from the sensors and stream them wirelessly to a smartphone companion app. (iii) BLE module for communication with a smartphone companion app. (iv) Battery circuitry to support diverse requirements of the above hardware components. Various hardware components were carefully assembled into a double-sided FPCB as shown in Fig. 4 to fit the form factor requirements. The hardware architecture is depicted in Fig. 3b. We redesigned NRF52832 [12] MCU which interfaces with the rest of the electronics based on the design of Sparkfun nRF52832 Breakout [66], as shown in the schematic diagram Fig. 2. The MCU consists of a 2.4

GHz radio frequency (RF) transceiver for BLE and ARM Cortex-M4 32-bit 64 MHz processor with floating-point unit (FPU) and supports multiple interfaces such as SPI, I2C, and UART. Such an SoC-based design choice results in a miniature MCU ($6\text{mm} \times 6\text{mm}$). The IMU chip incorporated is ICM20948 [5] which provides 9-axis IMU data and interfaces with the MCU using SPI. The PPG sensor incorporated is Maxim Integrated MAX30101 [7] which provides data using I^2C . The whole PCB is powered with a 15 mAh, 3.7V ring-shaped LiPo battery with a radius of 10.55 mm and thickness of 1.6 mm, which easily fits into the shape of a ring. Because the MCU requires 3.3 V whereas the IMU and PPG sensors require 1.8 V, we used an advanced dual low-drop-out (LDO) voltage regulator (MIC5370 [8]) for providing two independently-controlled power sources. Finally, we also integrate a circuit to protect PCB and battery from short current or overcharging. Overall, the power consumption of the hardware is about 12 mA when actively streaming the sensor data, and only about 76 μA under low power mode while the MCU is still collecting data and only streams the data periodically to the smartphone app. This provides sufficiently low power design to support a battery life of a week, thus enabling applications like sleep monitoring. In order to conveniently charge the smartring, we designed a charger based on Adafruit MicroLipo Battery Chargers [10]. The charger is connected to USB power source via the USB micro B cable, with charge rate of 1C.

Firmware and Phone

Application: The firmware of *OmniRing* includes three main components: (i) Collecting the data from the IMU and PPG sensors at the microcontroller; (ii) Packaging them into a packet; (iii) Sending the packets over BLE connection to a smartphone. We use C++, Arduino, and BLE libraries for implementing the functionalities [13, 14, 67]. The *OmniRing* Companion Application is an Android application that allows interaction with the sensors. The firmware and the phone app use popularly available Android and Arduino frameworks, thus can be easily extensible by developers to incorporate additional features.

Price Breakdown: Table 1 summarizes the retail and wholesale unit price for each major hardware component. All firmware packages and programs used to develop *OmniRing* will be made available at no cost. The total cost to produce a single *OmniRing* platform is as low as \$24.18, which is much lower than existing commercial products like OuraRing [57].

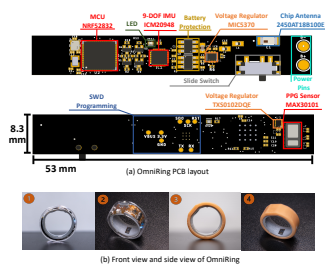


Figure 4: (a) Compute, sensing, communication, and power management circuitry as laid out on both sides of a FPCB that is later bent in the shape of a ring (b) Final *OmniRing* platform with the PCB enclosed in cases with either transparent or solid colors. Most users in our study preferred transparent cases for appearance.

Table 1: Manufacturing Cost Breakdown

Electronic Component	Unit Price (Retail) [U\$]	Unit Price (Wholesale) [U\$]
MCU (NRF52832)	5.02	2.23
PPG Sensor (MAX30101)	19.95	6.60
IMU Sensor (ICM20948)	26.45	6.63
Chip Antenna	0.59	0.23
Voltage Regulator ICs	1.47	0.80
Battery Protection ICs	0.32	0.18
Case (TPU&resin Filament)	0.01	0.01
Arc Battery	8.00	7.50
Total	61.81	24.18

4 USE CASE ANALYSIS

We provide a brief overview of potential use cases of *OmniRing*.

Mixed Reality in Metaverse: The idea of Metaverse includes a rich interconnection of real and virtual worlds where humans as avatars can interact with each other and software agents [54]. This was envisioned in the early 90s as a Sci-Fi concept. There is a recent push to make this vision a true reality by exploiting advances in high-speed internet, AI, computing, and sensing with several applications in areas like healthcare (remote surgery), education (collaborative learning), etc [17, 34]. We believe *OmniRing* can complement existing technology to make further inroads towards achieving this goal by providing insight into human activity and emotion levels. We also believe actuators can further be integrated into *OmniRing* in the future to provide a user with touch and haptic feedback.

Activity Monitoring: Personalized daily-life monitoring is popular nowadays to help people adapt an active and healthier lifestyle. With a form-factor that allows comfortable and long-time wearing, we believe *OmniRing* can help monitor daily life activities including running, eating, drinking, brushing, sleep cycles, etc [65].

Driving Behavior Monitoring: A useful case of behavior analytics is monitoring drivers' behavior [25]. By sensing the hand motion patterns with *OmniRing*, perhaps an alert system can be developed to identify risky or negligent driving and increase the safety. Similarly, *OmniRing* could also warn drivers from interacting with phones while driving.

Affective Computing and Behavior: Providing instructors with the ability to adapt the pedagogical content to the emotional state of students can make learning more engaging and fun [39]. *OmniRing* can potentially interpret students' emotional states by monitoring the interbeat intervals (IBI) of the heart as recorded by the PPG sensors. Also, the mental state of people with autism and depression can be constantly assessed, which can provide critical feedback to healthcare providers.

Accessibility Applications: We believe *OmniRing* can enable accessibility applications by helping people with special needs to interact or control devices. In the context of sign language recognition, we believe *OmniRing* can enable finger motion tracking to help recognize and translate sign languages to spoken languages to bridge the communication gap between deaf people and hearing people.

Health Monitoring: Daily-life health monitoring offers great benefits to users, especially those with heart diseases, hypertension, etc [22]. To this end, PPG sensors in *OmniRing* can

be used for monitoring of heart rate, blood pressure, and emotional states of users [24]. We believe this will not only help with better monitoring of diseases by providing fine-grained feedback to doctors but also has the potential to cut down medical expenses by decreasing visits to the hospital [81].

5 USER EXPERIENCE STUDY



Figure 5: User experience survey on *OmniRing* compared with three alternative sensing platforms

Our project is approved by the IRB. We conducted a user experience survey with participants who wore the sensor continuously under free-living conditions at their apartments. Each of 12 users wore several alternative platforms to *OmniRing* and compared the platforms with each other. We compare *OmniRing* with three other finger-based sensing or typing devices: Tapstrap [9], Myo [11], and CyberGlove [2]. The users conducted normal daily life activities including working on their laptops (typing, browsing, etc), eating, drinking, watching movies, etc, while wearing the sensor. Participants rated the four devices anonymously based on comfort, weight, and appearance from 0 to 10. Myo turned out to be rigid and not comfortable for long-time wearing and CyberGlove precludes finger motion that requires precision (cooking, typing, etc) apart from causing sweat. While Tapstrap received higher ratings than these two, users reported it as heavy and less comfortable for long-time wearing with restricted mobility of fingers due to the straps. *OmniRing* secured the highest scores in comfort, weight, and appearance as shown in Fig. 5. With the careful consideration of weight, and a form factor that allows daily life activities, we believe these results are not surprising, particularly given that a recent survey using a dummy ring also offers similar findings of social acceptance [20].

6 VALIDATION OF MOTION ANALYTICS: 3D FINGER MOTION TRACKING

While several possible applications were discussed earlier, we validate the capabilities of motion analytics in *OmniRing* by showing the feasibility of 3D finger motion tracking using IMU sensors. Particularly, we show the feasibility of tracking 24 DoFs of finger motion using sparse rings placed on a few fingers. This is an unconstrained problem without well-formed equations because the sensors are not placed on every finger or joint. Therefore, we utilize deep learning techniques to learn the mapping between sensor data and finger motion that exploit correlations between motion of different fingers to solve the underconstrained problem. However, unlike vision and speech domains with large quantities of training datasets, wearable devices, particularly newer ones like *OmniRing* have challenges in generating training datasets for developing robust machine learning algorithms. In solving this problem, Fig. 6 depicts *OmniRing*'s approach which synthesizes IMU training

data from videos and augments the data for 3D finger motion tracking. More details are elaborated next.

6.1 Background

Motivation: Wearable datasets are very small in comparison to their counterparts in computer vision. *Daphnet* [19] gait dataset only has 5 hours of walking IMU data from 10 subjects, and *PAMP2* dataset [60] only has 7.5 hours of sensor data from 9 subjects. Moreover to the best of our knowledge, such datasets do not exist for finger motion tracking using IMU. Thus, we synthesize IMU data from publicly available videos to transfer knowledge from the vision domain to the wearable domain, which alleviates the nontrivial cost of building *ImageNet*-like dataset for robust ML models of wearable.

Video Data: *OmniRing* identifies a public video dataset [30] that includes intricate and diverse finger motions by multiple users. It includes instructional videos on various activities like cooking, gardening, health, computers, exercise, etc in American Sign Language (ASL). We choose this dataset because the extremeness, complexity, and speed of finger motion patterns in these videos will subsume finger motion patterns in other applications like gaming and AR which are more simplistic. *OmniRing* extracts finger pose from these videos using Google *MediaPipe* [82]. Note that extracted locations may not be 100% accurate because fingers can get occluded. Although *MediaPipe* fills in some gaps in occlusions based on anatomical constraints, there might still be some frames where tracking is not possible. To this end, *OmniRing* uses simple interpolation and filtering to handle low-quality frames, which was sufficient to provide a stable accuracy for 3D finger motion tracking.

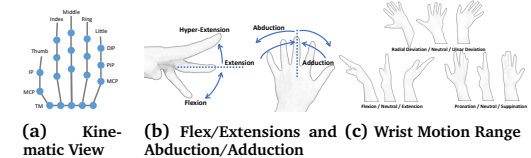


Figure 7: Kinematic view of hand and finger motion range, and wrist motion range

Finger skeletal model: Fig. 7a shows a kinematic view of finger joints. The four fingers excluding the thumb have four Degrees of Freedom (DoF) from the following finger joints: (i) MCP joint with two DoFs (Flex/extension - $\phi_{mcp,f/e}$ and abduction/adduction $\phi_{mcp,aa}$ as noted in Fig. 7b) (ii) PIP (ϕ_{pip}) and DIP (ϕ_{dip}) joints with a single DoF (Flex/extension). The thumb has slightly different anatomy as its MCP and TM joints can both flex/extend and abduct/adduct, and its IP (interphalangeal) joint can only flex/extend. Thus, the thumb has five

DoFs including $\phi_{mcp,f/e}$, $\phi_{mcp,a/a}$, $\phi_{tm,f/e}$, $\phi_{tm,a/a}$, and ϕ_{ip} , forming a 21-dimension (\mathbb{R}^{21}) space of joint angles with the other four fingers.

Wrist Motion: In addition to the fingers, we also track wrist motion. Fig. 7c depicts 3 DoFs of the wrist joint motion: i) pronation/supination, $\phi_{wrist,p/s}$; ii) flexion/extension, $\phi_{wrist,f/e}$; and iii) radial/ulnar deviation, $\phi_{wrist,r/u}$. As discussed earlier, the fingers and thumb have 21 DoFs whereas the wrist has 3 DoFs, totaling 24. *OmniRing* tracks these DoFs.

Hand Motion Constraints: Finger joints exhibit a high degree of correlation and interdependence [27, 49], some of which are detailed below.

$$\phi_{ip} = \frac{1}{2}\phi_{mcp,f/e}, \quad \phi_{dip} = \frac{2}{3}\phi_{pip}, \quad \phi_{mcp,f/e} = k\phi_{pip}, \quad 0 \leq k \leq \frac{1}{2} \quad (1)$$

Eq. 1 suggests that to bend the DIP joint, the PIP joint must also bend under normal finger motion (assuming no external force). Similarly, the range of motion for PIP is limited by the MCP joint. Besides, there is a range of motion constraints as follows:

$$-15^\circ \leq \phi_{mcp,aa} \leq 15^\circ, \quad 0^\circ \leq \phi_{dip} \leq 90^\circ, \quad 0^\circ \leq \phi_{pip} \leq 110^\circ$$

In addition, there are complex interdependencies between joints of different fingers, which cannot be directly modeled by equations, but our transformer architecture is designed to automatically learn such constraints.

6.2 Extraction of Synthetic IMU data

Extracting Synthetic Accelerometer Data: We first extract locations of finger joints and the wrist from videos. The location data is double differentiated with finite differences to approximate the accelerometer data. Thus, the synthetic accelerometer data from videos can be used for training. Fig. 8a shows an example of real accelerometer data and synthetic accelerometer data under a common frame of reference when a user is making a fist three times. Evidently, the two sources of data are similar indicating the feasibility of synthesizing accelerometer data from videos. Note that the gravity was subtracted from accelerometer measurements for this comparison by estimating the orientation of the sensor using techniques from A3 [85].

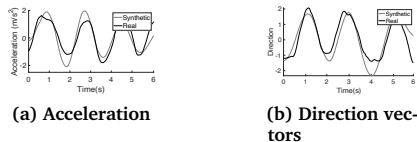


Figure 8: Synthetic data looks comparable with real data in y-axis

Extracting Synthetic Orientation Data: In addition to the accelerometer data, *OmniRing* also utilizes the orientation data from IMU sensors, a unit vector (y-axis in our settings) that follows finger directions. Towards this end, we identify the vector between MCP and PIP joints as a direction vector to capture the orientation. We ignored x- and z-axis direction vectors simply because the gain was negligible compared to the increase in the number of parameters in the ML model. Fig. 8b shows an example where synthetic direction vectors are compared to real ones, which indicates the feasibility of extracting synthetic orientation data from videos.

Body Size Standardization: It is easy to see that (i) Extraction of location in units of centimeters from videos needs camera parameters [53], which may not be available for public videos. (ii) Without camera parameters, the extracted locations from videos are in pixels, irrespective of user's body size. Therefore, we utilize body size standardization to handle differences in body sizes of users due to the lack of camera parameters [51].

6.3 Data Augmentation

To minimize the domain discrepancy between synthetic and real data, the synthetic training data is enhanced in size by performing the below-described data augmentation transformations. This also increases the diversity of the dataset thus making the ML models robust to extreme motion patterns, user diversity, variation in sensor position/orientation, etc.

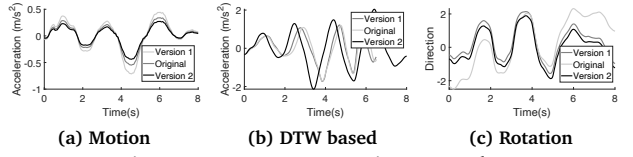


Figure 9: Data Augmentation Examples

Motion Enhancement: We enhance finger motion patterns extracted from the videos to vary the magnitude of flex/extensions and abduction/adductions. We believe it will enhance the coverage of finger motion distribution to account for all possible configurations in practice. While performing the augmentation, finger motion constraints (details in Sec. 6.1) are ensured, so that the augmented motion patterns are still realistic. Fig. 9a presents examples of such enhancements.

Dynamic Time Warping: We observed that (i) finger motion tends to be faster users when they are certain. Otherwise, finger motion is slower. (ii) Users perform motion at different speeds and the speed of motion can vary with time. To emulate such diversity in real IMU data and make ML models robust at inference, *OmniRing* utilizes *Dynamic Time Warping* (DTW) based augmentation to create augmented versions of the original data. Fig. 9b depicts examples of the original data being stretched and compressed.

Rotation Augmentation: Sensor position/orientation might vary under regular usage, particularly when the user removes and remounts the sensor rings multiple times in a day. Thus, we introduce perturbations in the direction vectors in the training data to increase the diversity of sensor position/orientation. Fig. 9c shows an example where the augmented data looks similar in shape to the original data but includes perturbations in the direction vectors.

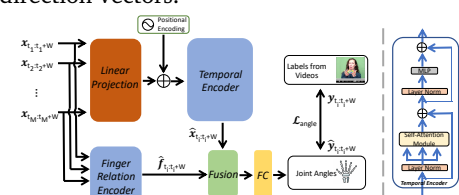


Figure 10: ML model processes inertial sensor input via two branches: (i) *Temporal Encoder* exploits time dependencies, (ii) *Finger Relation Encoder* leverages inter-finger correlations, and finally, two branches together contribute to hand pose prediction.

6.4 Learning based 3D Finger Motion Tracking

OmniRing's ML model for 3D finger motion tracking is depicted in Fig. 10. Our model can exploit temporal relationships and inter-finger correlations of finger motions. It consists of two branches: *Temporal Encoder* exploits dependencies across time and *Finger Relation Encoder* exploits dependencies across fingers. While *Temporal Encoder* employs *transformer* and *self-attention* mechanism that are efficient for processing series data in natural language processing and also in videos [28, 29, 72], *Finger Relation Encoder* is designed on the observation that finger motions exhibit rich inter-finger correlation. Experimental results (Sec. 6.7) suggest that both branches are critical in making inferences with sparse sensors on a high-dimensional search space (24 DoF). Details are elaborated next.

This design choice has other benefits over choices like CNNs (evaluated in Sec. 6.7) including: (i) In contrast to CNN, where spatial dependencies are a function of kernel sizes and network depth, and the ability to capture spatial dependencies depends on the distance between input elements, *transformer* captures spatial dependencies independent of the distance between input elements. This is relevant for applications in AR/VR and sports analytics, with a coordinated sequence of motions to achieve a specific task. (ii) Unlike *LSTM*, the attention values and data processing in *transformer* are amenable to parallelization, thus enhancing efficiency.

Input. The input data $\mathbf{x} \in \mathbb{R}^{C \times N}$, where $C = 36$ represents 6-dimensional input (acceleration and direction vectors) from sensors (fingers and wrist) and N denotes the number of time samples. To prepare input for *Temporal Encoder* and *Finger Relation Encoder*, we use a sliding window to generate M chunks along the time axis, $\mathbf{x}_{t_i:t_i+W} = \text{Chunk}(\mathbf{x}) \in \mathbb{R}^{C \times W}, i \in [1, M]$ and we select $W = 700$ empirically.

Temporal Encoder. To explore temporal dependencies, we employ a *Transformer Encoder* [72] as shown in Fig. 10. We embed the inputs, $\mathbf{x}_{t_i:t_i+W}$, by a Linear Projection (LP) layer and then positional information is added by a Positional Embedding layer (PE), which are later utilized in the *self-attention* layer of *Temporal Encoder* (TE) to encode dependencies (across time) into the learned representations $\hat{\mathbf{x}}_{t_i:t_i+W}$.

Finger Relation Encoder. The design of *Finger Relation Encoder* lies on a simple observation: finger motions are correlated as the motion of fingers can influence others (e.g., moving the middle finger most likely triggers the movement of the ring finger). To leverage the relation information across fingers, we perform below operations: Given the input $\mathbf{x}_{t_i:t_i+W} \in \mathbb{R}^{C \times W}$, we first reorganize the input $\mathbf{x}_{t_i:t_i+W} \in \mathbb{R}^{C \times W}$ into $\mathbf{x}'_{t_i:t_i+W} \in \mathbb{R}^{C' \times W'}$ where $C' = 6$ and $W' = \frac{C}{C'} \times W$. As wrist motion is independent of fingers, we only keep the inputs from 5 fingers to get $\mathbf{x}''_{t_i:t_i+W} \in \mathbb{R}^{(C'-1) \times W'}$. Secondly, we calculate the finger relation as follows.

$$\mathbf{f}_{t_i:t_i+W} = (\mathbf{x}''_{t_i:t_i+W})(\mathbf{x}''_{t_i:t_i+W})^T \in \mathbb{R}^{(C'-1) \times (C'-1)} \quad (2)$$

And lastly, we incorporate this information, $\mathbf{f}_{t_i:t_i+W}$, into our model by a *Multi-Layer Perceptron* (MLP) module to obtain the representation for finger relations $\hat{\mathbf{f}}_{t_i:t_i+W}$.

Branch Fusion and Output. The representations from the temporal encoder and the finger relation encoder are fused by a simple addition operation (we omit the validation details due to space limitation) and then passed a *Fully-Connected* (FC) layer to produce the final prediction of finger joint angles, $\hat{\mathbf{y}}_{t_i:t_i+W} \in \mathbb{R}^{18 \times W}$. Lastly, we concatenate all M chunks ($\hat{\mathbf{y}}_{t_i:t_i+W}$ and $\mathbf{y}_{t_i:t_i+W}$) to get $\hat{\phi} \in \mathbb{R}^{18 \times N}$ and $\phi \in \mathbb{R}^{18 \times N}$ for optimization. Among the 24 DoF finger joint angles discussed in Sec. 6.1, 18 joint angles are predicted by the model ($\mathbb{R}^{18 \times N}$ above) whereas the rest is inferred based on constraints with more details elaborated next with the description of the loss function.

Loss Function. As stated early, *OmniRing* aims to track finger motions instead of classifying. Therefore, we adopt Mean Square Error loss as our main loss. We define \mathcal{L}_{mse} as follows.

$$\mathcal{L}_{mse} = \sum_{j=1}^{j=18} (\hat{\phi}_j - \phi_j)^2 \quad (3)$$

In Equation 3, $\hat{\phi}_j$ denotes the prediction and ϕ_j denotes the training labels from videos. The $\hat{\phi}_j$'s above include MSE errors for: (i) Four flex/extension angles of MCP joint from four fingers (excluding thumb) (ii) Four MCP adduction/abduction angles of the MCP joint from four fingers ($\hat{\phi}_{j,mcp,aa} \forall j \in [1, 4]$) (iii) Four PIP joint angles from four fingers ($\hat{\phi}_{j,PIP} \forall j \in [1, 4]$) (iv) Flex/extension and abduction/adduction angles of MCP and TM joints of the thumb, a total of four angles ($\phi_{mcp,f/e}, \phi_{mcp,a/a}, \phi_{tm,f/e}, \phi_{tm,a/a}$) (v) Flex/extension and Radial/ulnar deviation angles of the wrist ($\phi_{wrist,r/u}, \phi_{wrist,f/e}$). In addition, to encourage the similarity of the overall shapes of ϕ_j and $\hat{\phi}_j$, we incorporate a cosine similarity loss into our loss function.

$$\mathcal{L}_{CosineSimilarity} = \sum_{j=1}^{j=18} \frac{\hat{\phi}_j \cdot \phi_j}{\max(||\hat{\phi}_j||_2 \cdot ||\phi_j||_2, \epsilon)}, \quad \epsilon = 10^{-6} \quad (4)$$

The overall loss function is now expanded below.

$$\mathcal{L}_{angle} = \mathcal{L}_{mse} + \alpha \mathcal{L}_{CosineSimilarity} \quad (5)$$

where we set α to 0.4 empirically.

Note that the loss function (Eq. 5) does not include ϕ_{dip} , or ϕ_{ip} because we compute them directly from anatomical constraints in [27, 49] (more details in Sec. 6.1). The pronation/supination angle ($\phi_{wrist,p/s}$) for the wrist is also directly computed from the orientation of the wrist sensor [63].

6.5 User Study

Data Collection Methodology: Since there is no publicly available IMU dataset for finger motion tracking, we collect our own dataset using the platform described in Sec. 3. The collected real IMU data is only for testing. The training data is extracted from sources of online videos as identified in Sec. 6.1. Our study has been approved by the IRB. We conducted a study with 12 users (8 males, 4 females), aged between 20-47 and weighing between 44-105 kgs. For stress testing *OmniRing* across all possible hand poses, we follow the guidelines from the literature [49] to cover an exhaustive space of all possible hand poses. The majority of possible hand poses are known to be one of these *base states* or transitioning between these poses [69] based on anatomical feasibility constraints. The

users are allowed to make natural and random finger motions while ensuring that the above base states are included in their motion pattern in random order. This ensures good coverage by incorporating the entire range of motion of possible hand poses. Each user participates in 5 sessions of 5 mins while removing and remounting the sensor across sessions to validate robustness to natural changes in sensor positions and orientation. Wrist and arm mobility is varied across sessions as indicated in Fig. 11. The accuracy was also studied for longer duration free-living experiments.

Labels for Validation:

The collected data includes 9-axis IMU and the fingers' 3D coordinates and joint angles are captured by the Leap depth camera [1]. The IMU data provides motion data for 3D finger tracking. The leap data serves as ground truth. We note that Leap has location tracking error $< 0.2\text{mm}$ [79], thus sufficient for ground truth. Since *OmniRing* performs continuous finger tracking instead of discrete gesture classification, we employ the loss function defined in Eq. 5 in our system.

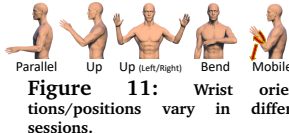


Figure 11: Wrist orientations/positions vary in different sessions.

6.6 Implementation

The ML model is implemented with Pytorch. The training is done on a desktop with Intel i7-8700K CPU, 32GB RAM, and an NVIDIA RTX 2080 GPU. We use Adam optimizer [45] (β_1 of 0.9, β_2 of 0.98), a varied learning rate based on [72]. To avoid overfitting, we apply the L2 regularization (parameter of 0.01) and a dropout rate (parameter of 0.5) following each layer. Once trained, the inference is done on smartphones (Samsung S20, OnePlus 9 Pro) using Pytorch Mobile [31].

6.7 Motion Tracking Performance

To assess the performance of *OmniRing*, we conduct the following analysis:

- Since no public datasets exist for IMU-based 3D finger motion tracking, we perform a comparison with naive baselines including ablation studies. This validates the importance and effectiveness of design choices of *OmniRing*.
- We conduct robustness studies to characterize the performance of *OmniRing* over accuracy vs fingers, users, number of sensors, and long durations (ability to handle sensor drifts).
- We provide a qualitative reconstruction of hand poses and compare the results to the ground truth.
- We evaluate the power consumption and latency on smartphones when executing ML models.
- Finally, we contrast features and accuracy of *OmniRing* with prior work.

6.7.1 Ablation Studies.

Ablation Study of Baselines: We convert joint angle errors to position errors and present position error (millimeters) for most results. Table 2 shows *OmniRing* against three baselines.

- **CNN-LSTM-based Model:** We build a CNN-LSTM-based model for the same tracking problem to verify that the design of *OmniRing*'s ML model is effective in capturing temporal relations for time-series data. In comparison to this design, we

observe that *OmniRing* reduces the error by 20.4% and 23.2% for median and mean location error respectively. ■ **w/o Cosine Similarity Loss:** The results show, by encouraging similar shapes of the output and the ground truth with Eq. 4, the location error decreases by 16.4% and 9.2% for median and mean respectively. ■ **w/o Finger Relation Encoder:** *FRE* as in Sec. 6.4 aims to take finger relations into consideration. To test its effectiveness in tracking 3D finger motions, we build a model without this module. *FRE* improves the accuracy by 20.4% and 18.2% for median and mean location error respectively.

Ablation Study of Data Augmentation: We also study the effectiveness of individual data augmentations in *OmniRing* as shown in Table 2. ■ **Motion Enhancement** decreases mean location error by 5%, which shows the effectiveness of increasing the coverage of finger motion distribution in reality. ■ **DTW Augmentation** also improves performance by a similar degree, by incorporating different speeds of different parts of finger motion into the training data. ■ **Rotation Augmentation** emulates the diversity of wearing positions in daily life, and improves *OmniRing* by 4.6% for mean location error. Overall, the combination of all three data augmentation techniques boost the performance of *OmniRing* by 24.1% and 23.2% for median and mean location errors respectively, which demonstrates that *OmniRing* can acquire knowledge from a different domain with the help of simple but effective data augmentation methods, and henceforth mitigate the need of large-scale IMU datasets.

6.7.2 Robustness Studies.

Accuracy vs Fingers and Wrist is depicted in Fig. 12a. Synthetic training data and data augmentation transformations incorporate the full range of motion across fingers and wrist, enabling accurate tracking of all fingers and wrist.

Accuracy vs Users: Depicted in Fig. 12b, *OmniRing* achieves consistent accuracy across users with minor variations. The variation happens because some users perform faster motions. Nevertheless, the user with the worst performance only has $\approx 1\text{ mm}$ (1.35°) higher error than average. Given the diverse sources from which the synthetic training data was generated with the added diversity via data augmentations, we believe *OmniRing* generalizes to a variety of users.

Accuracy vs. Number of Sensors is depicted in Fig. 12c. The position of sensors for each case is also indicated. The ML model input shape in Sec. 6.4 was appropriately adjusted to work with sparse sensors. There is a graceful degradation in accuracy with fewer sensors. With a high degree of interaction between fingers, the motion of one finger will cause other fingers to move, thus enabling tracking them even without sensor rings on all fingers, which can further enhance the comfort levels of wearing.

Longer Session Experiments (Free-Living Conditions): We conducted *free-living* experiments to study long-term effects like potential drifts. Users were instructed to wear the sensor continuously for 6 hours at their apartments. At the end of each hour, we conduct a 5-minute session of finger motion as per our user study protocol described earlier. In between sessions, the users conducted daily activities including working on their laptops (typing, browsing, etc), eating, drinking,

Model	Baselines Comparisons (errors in millimeters)					
	50%-ile Error	90%-ile Error	Mean	STD	Median Absolute Dev	Mean Absolute Dev
CNN-LSTM-based Model	8.25	21.65	10.32	8.78	4.74	6.46
w/o Cosine Similarity Loss	7.86	17.14	8.73	5.69	3.03	4.25
w/o Finger Relation Encoder	8.25	19.99	9.70	6.58	3.53	5.07
<i>OmniRing</i> (Ours)	6.57	17.10	7.93	5.85	2.98	4.44

Model	Data Augmentation Study (errors in millimeters)					
	50%-ile Error	90%-ile Error	Mean	STD	Median Absolute Dev	Mean Absolute Dev
w/o Data Aug.	8.66	22.47	10.63	7.81	4.16	6.02
Only Motion Enhancement	6.81	18.49	8.35	6.42	3.23	4.88
Only DTW Aug.	6.84	18.29	8.35	6.27	3.10	4.74
Only Rotation Aug.	6.61	18.75	8.31	6.53	3.14	4.98
<i>OmniRing</i> (Ours)	6.57	17.10	7.93	5.85	2.98	4.44

Table 2: We present the effectiveness of different components in our ML model. In a nutshell, *Finger Relation Encoder* improves the performance by 20.4% and data augmentation techniques boost the tracking accuracy by 24.1%. More details are presented in the text.

watching movies, etc., while wearing the sensor. The results are depicted in Fig. 12d. As expected, the accuracy does not degrade with time. This is because *OmniRing* does not perform long-term integration of data, which is the main source of drift errors [76]. In contrast, *OmniRing* opportunistically resets drifts, and eliminates magnetic interference based on A3 [85].

6.7.3 Qualitative Results.

Fig. 13 depicts the qualitative results. The figure compares the tracking of hand poses by *OmniRing* with reference to the real hand and ground truth (from Leap). Evidently, *OmniRing* can capture a wide range of finger motions with decent accuracy, even without the need to place sensor rings on all fingers by exploring the inter-finger correlations. Overall, we believe these results are promising in the context of applications in activity tracking, sport analytics, etc.

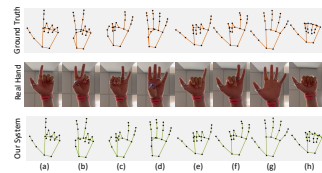


Figure 13: Qualitative tracking results show that *OmniRing* tracks hand poses closely even without placing sensor rings on all fingers.

6.7.4 Power Consumption and Latency. To make *OmniRing* real-time, at any given instant of time, we feed previous few chunks to the ML model. The latency of execution on Samsung S20 and OnePlus 9 Pro are around 8.4 ms and 7.6 ms respectively, sufficient for real-time applications. The real-time power discharge rate is 14.43% and 16.72% per hour for Samsung S20 and OnePlus 9 Pro, while the discharge rate under the low-power mode is around 6% for both models.

6.7.5 Comparison with Vision and other Wearables: *OmniRing* achieves a tracking error of 6.57mm, while work such as WR-Hand [52] has an error of 18.57mm, FingerTrak [40] achieves an error of 9.44mm, and a pure camera-based [23] has an error of 14.2mm. Note that this might not be a fair comparison as the hardware, sensor data, etc., is different, and the respective datasets and customized hardware is not publicly available yet in all cases. Nevertheless, we believe its promising that *OmniRing*'s accuracy is comparable to prior efforts while

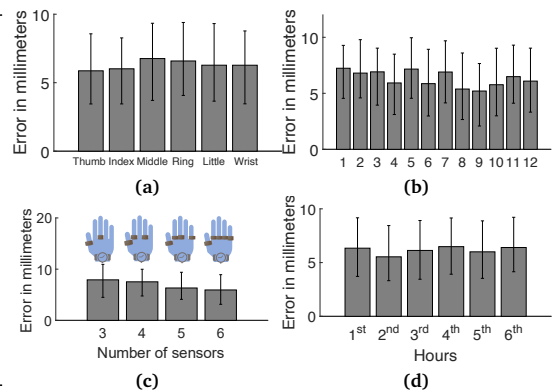


Figure 12: (a) Accuracy over Fingers and Wrist (b) Accuracy over Users (c) Accuracy degrades gracefully with lesser sensors (d) Error does not accumulate over long-duration and free-living experiments

offering additional benefits over prior works as identified in Sec. 2 such as providing a ubiquitous, comfortable, and more privacy-preserving solution while being agnostic to lighting, background, and other ambient conditions.

7 PRELIMINARY VALIDATION OF HEALTH ANALYTICS: HEART RATE ESTIMATION

For the sake of completeness, we conduct a basic feasibility of extraction of raw PPG data from *OmniRing* for heart rate estimation. A discussion of other use cases of PPG was provided in Sec. 4 and we leave a thorough investigation of this space for future work. *OmniRing* is incorporated with a PPG sensor for health related sensing tasks such as heart rate, SpO_2 , etc. A PPG sensor illuminates the skin and measures the absorption which can be used for detecting blood volume changes in the subcutaneous tissues of the skin due to the pumping of blood during the cardiac cycle. Therefore by measuring the absorption, metrics like heart rate and blood pressure can be computed [24]. To validate the PPG data, we conducted a preliminary study for heart rate monitoring, in which we asked users to perform simple activities (i.e., standing, sitting, running, and standing) and collected PPG data for estimating the heart rates. Fig. 14a shows an example of PPG data that is processed by a bandpass filter and biometric characteristics (e.g., Systolic/Diastolic peaks, IBI, etc) denoted in the figure can be utilized to monitor heart rates. We estimated the heart rates when users remain static after each activity and Fig. 14b depicts *OmniRing* monitors heart rates closely.

In addition, we studied heart rate monitoring accuracy for individuals as shown in Fig. 14c. Overall, the heart rate estimation is stable across different users. Worthy noting that our users not only span a various range of ages and body shapes but also cover different skin tone colors. However, we don't see significant difference between light and dark skin tones. Our findings are consistent with recent research [21, 59]. We believe this preliminary study has demonstrated that *OmniRing* has the potential to enable healthcare applications in addition to motion tracking. We hope the community will use the platform to explore more specific uses cases of the PPG sensor.

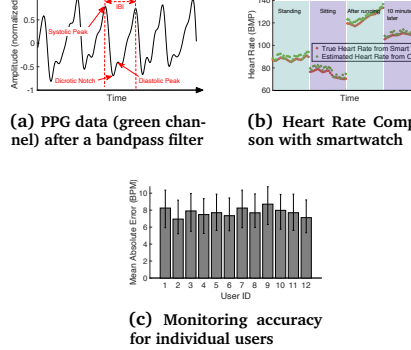


Figure 14: *OmniRing* can also monitor heart rate closely.

8 DISCUSSION AND FUTURE WORK

Extensibility of *OmniRing* to Incorporate Additional Sensors: This paper shows the feasibility of incorporating IMU and PPG sensors in the current *OmniRing* design. While IMU can be used in several applications in activity recognition, the PPG sensor can be used in health analytic applications including heart rate, sleep, and emotion monitoring. However, we believe we have only scratched the surface. Additional sensors such as ECG and EDA can be incorporated for applications in heart disease detection and stress levels. Moreover, integrating touch and haptic sensors can enable feedback to the user in applications like gaming. While the space might be limited to include all sensors in one ring, different sensing modalities can be integrated into different rings if the user is willing to wear rings on multiple fingers. We are currently exploring these tradeoffs and we hope that the community can extend our platform to enable exciting new possibilities.

On-Device Computing: The MCU in *OmniRing* currently sends the sensor data to a smartphone app for analytics. However, given that the CPU (ARM's Cortex-M4) can support signal processing and machine learning [78], we will consider the tradeoffs between on-device computing/preprocessing and offloading the sensor data as a part of our future work.

Authentication and Biometry: While we focus on motion analytics and healthcare applications in this paper, we believe the platform can be extended for applications in biometric authentication. For example, the heartbeat pattern is known to be a fingerprint that is characteristic of a person [77]. The heart rate estimation from the PPG sensor in *OmniRing* can be exploited for authenticating an individual.

9 CONCLUSION

OmniRing shows the feasibility of designing a low cost ($\approx \$25$) smartring by exploiting advances in SoC, flexible PCB and 3D printed materials in creating a device with a small form-factor and long battery life, comfortable for wearing day and night. IMU and PPG sensors were embedded within *OmniRing* to enable an array of diverse applications in motion analytics and healthcare. While the IMU sensors can enable applications like activity tracking, sports analytics, and augmented reality, the PPG sensor can enable applications like monitoring of heart rate, blood pressure, emotion and sleep. A user experience

study was conducted that indicates the acceptability and comfort levels of *OmniRing* for wearing in daily life. To validate the sensing capabilities of *OmniRing*, we enable an application in 3D finger motion tracking. While generating training data could be an overhead for new wearable devices, synthetic training data was extracted from public videos and enhanced with data augmentation. A transformer based machine learning model was designed to exploit correlations across fingers and time to enable accurate tracking without placing sensors on all fingers. Finally, a basic validation of use of PPG sensors in an application in heart rate monitoring was provided. Despite promise, we believe we only scratch the surface. Our platform is fully extensible and we believe the community can expand *OmniRing* with additional hardware and software capabilities.

ACKNOWLEDGMENTS

This research was partially supported by NSF grants: CAREER-2046972, CNS-1909479, and CNS-2008384.

REFERENCES

- [1] 2012. Leap Motion. <https://developer.leapmotion.com/>.
- [2] 2017. CyberGlove. <http://www.cyberglovesystems.com/>.
- [3] 2018. Smart Rings Market Is Booming. <https://www.globenewswire.com/news-release/2022/03/21/2406423/0/en/Smart-Rings-Market-Is-Booming-Worldwide-with-a-CAGR-of-28.9-During-2022-2028-Growth-Factors-Product-and-Service-Investment-Plans-Future-Strategic-Planning-Drivers-Trends-Challenges.html>.
- [4] 2019. OuraRing - What we learned about the sleep tracking ring. <https://www.cnbc.com/2019/12/20/oura-ring-review---what-we-learned-about-the-sleep-tracking-ring.html>.
- [5] 2021. ICM20948 datasheet. <https://3cfeqx1hf82y3xcoull08ihx-wpgenie.netdna-ssl.com/wp-content/uploads/2021/10/DS-000189-ICM-20948-v1.5.pdf>.
- [6] 2021. Kinect2.0. <https://developer.microsoft.com/en-us/windows/kinect>.
- [7] 2021. MAX30101. <https://www.mouser.com/new/maxim-integrated/maxim-max30101-sensor/>.
- [8] 2021. MIC3570 datasheet. <https://www.microchip.com/en-us/product/MIC3570>.
- [9] 2021. TapStrap 2. <https://www.tapwithus.com/>.
- [10] 2022. Adafruit MicroLipo and MiniLipo Battery Chargers. <https://learn.adafruit.com/adafruit-microlipo-and-minilipo-battery-chargers>.
- [11] 2022. Myo tutorial. <https://learn.adafruit.com/myo-armband-teardown>.
- [12] 2022. NRF52832. <https://www.nordicsemi.com/products/nrf52832>.
- [13] Adafruit. 2021. Bluefruit nRF52 Feather Learning Guide. <https://learn.adafruit.com/bluefruit-nrf52-feather-learning-guide>.
- [14] Adafruit. 2021. ICM20X. https://github.com/adafruit/Adafruit_ICM20X.
- [15] D Agrò et al. 2014. PPG embedded system for blood pressure monitoring. In *AET*.
- [16] Mohamed Aktham Ahmed et al. 2018. A review on systems-based sensory gloves for sign language recognition state of the art between 2007 and 2017. *Sensors* 18, 7 (2018), 2208.
- [17] Hosam Al-Samarraie et al. 2018. A systematic review of cloud computing tools for collaborative learning: Opportunities and challenges to the blended-learning environment. *Computers & Education* 124 (2018), 77–91.
- [18] Amento et al. 2002. The sound of one hand: A wrist-mounted bio-acoustic fingertip gesture interface. In *CHI*.
- [19] Marc Bachlin et al. 2009. Wearable assistant for Parkinson's disease patients with the freezing of gait symptom. *IEEE Transactions on Information Technology in Biomedicine* 14, 2 (2009), 436–446.
- [20] Sandra Bardot et al. 2022. One Ring to Rule Them All: An Empirical Understanding of Day-to-Day Smartring Usage Through In-Situ Diary Study. *ACM IMWUT* (2022).
- [21] Brinnae Bent et al. 2020. Investigating sources of inaccuracy in wearable optical heart rate sensors. *NPJ digital medicine* 3, 1 (2020), 1–9.
- [22] Lora E Burke et al. 2015. Current science on consumer use of mobile health for cardiovascular disease prevention: a scientific statement from the American Heart Association. *Circulation* 132, 12 (2015), 1157–1213.
- [23] Zhe Cao et al. 2021. Reconstructing hand-object interactions in the wild. In *CVPR*. 12417–12426.

- [24] Denisse Castaneda et al. 2018. A review on wearable photoplethysmography sensors and their potential future applications in health care. *International journal of biosensors & bioelectronics* 4, 4 (2018), 195.
- [25] Teck Kai Chan et al. 2019. A comprehensive review of driver behavior analysis utilizing smartphones. *IEEE Transactions on Intelligent Transportation Systems* 21, 10 (2019), 4444–4475.
- [26] Yujin Chen et al. 2021. Model-based 3d hand reconstruction via self-supervised learning. In *Proceedings of CVPR*. 10451–10460.
- [27] Fai Chen Chen et al. 2013. Constraint study for a hand exoskeleton: human hand kinematics and dynamics. *Journal of Robotics* (2013).
- [28] Jacob Devlin et al. 2018. Bert: Pre-training of deep bidirectional transformers for language understanding. *arXiv preprint* (2018).
- [29] Alexey Dosovitskiy et al. 2020. An image is worth 16x16 words: Transformers for image recognition at scale. *arXiv preprint* (2020).
- [30] Amanda Duarte et al. [n. d.]. How2Sign: a large-scale multimodal dataset for continuous American sign language. In *IEEE CVPR*.
- [31] Facebook. 2021. Introduce lite interpreter workflow in Android and iOS. "<https://pytorch.org/mobile/android/>".
- [32] Nazli FarajiDavar et al. 2011. Transductive transfer learning for action recognition in tennis games. In *ICCV Workshops*. IEEE, 1548–1553.
- [33] Finch Ring 2022. <https://finchxr.com/>.
- [34] Danilo Gasques et al. 2021. ARTEMIS: A collaborative mixed-reality system for immersive surgical telementoring. In *CHI*.
- [35] Bogdan-Florin Gheran et al. 2018. Gestures for smart rings: Empirical results, insights, and design implications. In *DIS*.
- [36] Teng Han et al. 2017. Frictio: Passive kinesthetic force feedback for smart ring output. In *UIST*.
- [37] Nikolas Hesse et al. 2018. Computer vision for medical infant motion analysis: State of the art and rgb-d data set. In *ECCV*.
- [38] Trung-Hieu Hoang et al. 2022. Towards a Comprehensive Solution for a Vision-based Digitized Neurological Examination. *IEEE Journal of Biomedical and Health Informatics* (2022).
- [39] Danial Hooshyar et al. 2019. Mining educational data to predict students' performance through procrastination behavior. *Entropy* 22, 1 (2019), 12.
- [40] Fang Hu et al. 2020. FingerTrak: Continuous 3D Hand Pose Tracking by Deep Learning Hand Silhouettes Captured by Miniature Thermal Cameras on Wrist. *ACM IMWUT* (2020).
- [41] Yinghao Huang et al. 2018. Deep inertial poser: learning to reconstruct human pose from sparse inertial measurements in real time. *ACM TOG* (2018).
- [42] Syed Anas Imtiaz. 2021. A systematic review of sensing technologies for wearable sleep staging. *Sensors* (2021).
- [43] Wolf Kienzle et al. 2014. LightRing: always-available 2D input on any surface. In *UIST*. 157–160.
- [44] David Kim et al. 2012. Digits: freehand 3D interactions anywhere using a wrist-worn sensor. In *ACM UIST*.
- [45] Diederik P Kingma et al. 2014. Adam: A method for stochastic optimization. *arXiv preprint arXiv:1412.6980* (2014).
- [46] Hyeokhyen Kwon et al. 2020. IMUTube: Automatic extraction of virtual on-body accelerometry from video for human activity recognition. *ACM IMWUT* 4, 3 (2020), 1–29.
- [47] Hyeokhyen Kwon et al. 2021. Approaching the Real-World: Supporting Activity Recognition Training with Virtual IMU Data. *ACM IMWUT* (2021).
- [48] Chen Liang et al. [n. d.]. DualRing: Enabling Subtle and Expressive Hand Interaction with Dual IMU Rings. *ACM IMWUT* 5, 3 ([n. d.]).
- [49] John Lin and others. 2000. Modeling the constraints of human hand motion. In *Proceedings workshop on human motion*. IEEE, 121–126.
- [50] Yilin Liu et al. 2021. NeuroPose: 3D Hand Pose Tracking using EMG Wearables. In *WWW*. 1471–1482.
- [51] Yilin Liu et al. 2021. When Video meets Inertial Sensors: Zero-shot Domain Adaptation for Finger Motion Analytics with Inertial Sensors. In *IoTDI*.
- [52] Yang Liu et al. 2021. WR-Hand: Wearable Armband Can Track User's Hand. *ACM IMWUT* 5, 3 (2021), 1–27.
- [53] Franziska Mueller et al. 2018. Generated hands for real-time 3d hand tracking from monocular rgbs. In *IEEE CVPR*.
- [54] Stylianos Myskakidis. 2022. Metaverse. *Encyclopedia* 2, 1 (2022), 486–497.
- [55] Shahriar Nirjon et al. 2015. Typingring: A wearable ring platform for text input. In *ACM MobiSys*.
- [56] Kenji Oka et al. 2002. Real-time fingertip tracking and gesture recognition. *IEEE Computer graphics and Applications* 22, 6 (2002), 64–71.
- [57] OuraRing 2021. <https://ouraring.com/>.
- [58] Farshid Salemi Parizi et al. 2019. AuraRing: Precise Electromagnetic Finger Tracking. *ACM IMWUT* (2019).
- [59] Ishita Ray et al. 2021. Skin tone, confidence, and data quality of heart rate sensing in WearOS smartwatches. In *PerCom Workshops*.
- [60] Attila Reiss et al. 2012. Introducing a new benchmarked dataset for activity monitoring. In *IEEE ISWC*. 108–109.
- [61] Vitor Fortes Rey et al. 2019. Let there be IMU data: generating training data for wearable, motion sensor based activity recognition from monocular RGB videos. In *ACM UbiComp/ISWC*. 699–708.
- [62] Alba Roda-Sales et al. 2020. Effect on manual skills of wearing instrumented gloves during manipulation. *Journal of biomechanics* (2020).
- [63] Sheng Shen et al. 2016. I am a Smartwatch and I can Track my User's Arm. In *ACM MobiSys*.
- [64] Sherin Shibu. 2022. Ditch the fitness tracker on your wrist and get a smart ring instead. <https://www.zdnet.com/article/best-smart-ring/>.
- [65] Grace Shin et al. 2019. Wearable activity trackers, accuracy, adoption, acceptance and health impact: A systematic literature review. *Journal of biomedical informatics* 93 (2019), 103153.
- [66] SparkFun. 2021. nRF52832 Breakout-WRL-13990. <https://www.sparkfun.com/products/retired/13990>.
- [67] Sparkfun. 2021. SparkFun MAX301x Particle Sensor Library. https://github.com/sparkfun/SparkFun_MAX3010x_Sensor_Library.
- [68] Shingo Takeda et al. 2018. A multi-sensor setting activity recognition simulation tool. In *ACM UbiComp*. 1444–1448.
- [69] Carlo Tomasi et al. 2003. 3D Tracking=Classification+Interpolation. In *ICCV*.
- [70] Catherine Tong et al. [n. d.]. Zero-Shot Learning for IMU-Based Activity Recognition Using Video Embeddings. *ACM IMWUT* 5, 4 ([n. d.]).
- [71] Hoang Truong et al. 2018. CapBand: Battery-free Successive Capacitance Sensing Wristband for Hand Gesture Recognition. In *ACM SenSys*.
- [72] Ashish Vaswani et al. 2017. Attention is All You Need. In *NeurIPS*.
- [73] Radu-Daniel Vatavu et al. 2021. GestuRING: A web-based tool for designing gesture input with rings, ring-like, and ring-ready devices. In *ACM UIST*.
- [74] Manuel Vázquez-Enríquez et al. 2021. Isolated sign language recognition with multi-scale spatial-temporal graph convolutional networks. In *Proceedings of CVPR*. 3462–3471.
- [75] ViCON MoCap 2020. <https://www.vicon.com/>.
- [76] He Wang et al. 2012. No need to war-drive: Unsupervised indoor localization. In *MobiSys* 2012. 197–210.
- [77] Lei Wang et al. 2018. Unlock with your heart: Heartbeat-based authentication on commercial mobile phones. *ACM IMWUT* (2018).
- [78] Pete Warden et al. 2019. *TinyML: Machine learning with tensorflow lite on arduino and ultra-low-power microcontrollers*. O'Reilly Media.
- [79] Frank Weichert et al. 2013. Analysis of the accuracy and robustness of the leap motion controller. *Sensors* 13, 5 (2013), 6380–6393.
- [80] Erwin Wu et al. 2020. Back-Hand-Pose: 3D Hand Pose Estimation for a Wrist-worn Camera via Dorsum Deformation Network. In *ACM UIST*.
- [81] Stephanie WY Yu et al. 2017. The scope and impact of mobile health clinics in the United States: a literature review. *International journal for equity in health* 16, 1 (2017), 1–12.
- [82] Fan Zhang et al. 2020. Mediapipe hands: On-device real-time hand tracking. *arXiv preprint arXiv:2006.10214* (2020).
- [83] Shibo Zhang et al. [n. d.]. Deep generative cross-modal on-body accelerometer data synthesis from videos. In *ACM IMWUT*.
- [84] Hao Zhou et al. 2022. Learning on the Rings: Self-Supervised 3D Finger Motion Tracking Using Wearable Sensors. *ACM IMWUT* (2022).
- [85] Pengfei Zhou et al. 2014. Use it free: Instantly knowing your phone attitude. In *ACM MobiCom*.